Per. Mineral. (2006), *75*, 2-3, 95-112 http://go.to/permin

PERIODICO di MINERALOGIA
established in 1930

An International Journal of
MINERALOGY, CRYSTALLOGRAPHY, GEOCHEMISTRY, ORE DEPOSITS, PETROLOGY, VOLCANOLOGY
and applied topics on *Environment*, *Archaeometry* and *Cultural Heritage*

Technology and Provenance of roman ceramics from Scoppieto, Italy: a mineralogical and petrological study

Paola Comodi[1*], Sabrina Nazzareni[1], Diego Perugini[1], Margherita Bergamini[2]

[1] Dipartimento di Scienze della Terra, Università di Perugia, 06100 Perugia, Italy
[2] Dipartimento di Scienze Storiche, Università di Perugia, 06100 Perugia, Italy

Abstract. — Scoppieto (Terni, Italy) was an important centre devoted mainly to the production of *terra sigillata* vessels, lamps, and probably utilitarian pottery in the Augustean period-production, which increased sharply from the Tiberian period onwards. Several findings of coarse ware (*Opus Doliare*, amphorae) suggest that the site may have been active in the production of common ceramics before that of the "*Terra Sigillata Italica*". However whether these materials were imported or produced on site was completely unknown until now.

A collection of coarse ware, of both good quality and waste products, were characterised by mineralogical (Rietveld and calorimetric analyses) and petrological analytical techniques (XRF, LA-ICP-MS), to investigate production techniques and provenance.

Rietveld analysis indicated differing contents of amorphous contents from 17% to 52%, with a mineralogical association always constituted of quartz, feldspar, plagioclase and pyroxenes, and in some cases by phyllosilicates and calcite. Considerable weight loss variations, from 0.5% to 8%, are associated with the presence of calcite and phyllosilicates. Generally, the highest weight losses were measured in the good-quality products, whereas waste products turned out to have been fired at higher temperatures than those of the breakdown of calcite and phyllosilicates.

The chemical and mineralogical compositions of good-quality ceramic objects and those of waste products indicate that the unsuccessful process, which produced a large quantity of discarded materials, was due to poor control of firing temperature, not to mistakes in the mixture. Trace element abundances in good-quality and waste products are similar, indicating local production and favouring the hypothesis that Scoppieto was active since pre-Augustean times.

Further constraints to this hypothesis are given by a detailed study of clinopyroxene crystals of igneous origin occurring in all the studied ceramics, compared with the chemical features of the same mineral phase present in volcanic rocks of the nearby Roman Magmatic Province. Geochemical results indicate that the rocks of the Bolsena Volcanic Complex, located near the Scoppieto production site, were probably the volcanic starting materials, used as refractory components in the ceramics examined here.

Key Words: *ceramics, technology, provenance, Roman Ages, Italy, Rietveld Analysis, LA-ICP-MS.*

Riassunto. — Il sito Archeologico di Scoppieto (Terni, Italia) è stato un importante centro votato principalmente alla produzione di vasellame in "*Terra Sigillata*", di lucerne e probabilmente di ceramica comune nel periodo Augusteo, registrando un forte incremento dall'età di Tiberio. Diversi ritrovamenti datati pre-augustei di ceramica grossolana (*Opus Doliare*, anfore) hanno suggerito che il sito potesse essere già attivo per la produzione di ceramica

* Corresponding author, E-mail: comodip@unipg.it

comune prima della produzione di "*Terra Sigillata Italica*". Rimane ancora incerto se questi materiali fossero importati o fossero prodotti locali.

Una serie di ceramiche grossolane, sia ben fatte che scarti di produzione sono stati caratterizzati con tecniche mineralogiche (analisi Rietveld e calorimetriche) e petrologiche (XRF e LA-ICP-MS) per investigare le tecniche di produzione e la provenienza.

Le analisi Rietveld hanno suggerito un diverso contenuto di amorfo da 17 a 52%, e le associazioni mineralogiche costituite sempre da quarzo, feldspati, plagioclasi e pirosseni, in alcuni casi da fillosilicati e calcite. Rilevanti variazioni nelle analisi termiche, da 0.5 a 8%, sono state associate alla presenza di calcite e fillosilicati. In generale, le più grosse perdite in peso sono state misurate nei campioni ben fatti, mentre per gli scarti è risultata una temperatura di cottura più alta di quella di decomposizione della calcite e dei fillosilicati.

Le composizioni chimiche e mineralogiche delle ceramiche ben fatte e quelle degli scarti sono simili e indicano che la mal riuscita dei processi che ha prodotto una grossa quantità di materiale di scarto è dovuta ad uno scarso controllo della temperatura di cottura piuttosto che ad erronee composizioni della miscela di partenza. La similarità della distribuzione degli elementi in traccia dei prodotti ben fatti e degli scarti, indicano che il sito produttivo di Scoppieto potesse essere stato attivo già prima dell'età augustea.

Ulteriori prove di questa ipotesi sono emerse dallo studio di cristalli di clinopirosseni di origine ignea presenti in tutte le ceramiche studiate, comparato con le caratteristiche chimiche della stessa fase minerale presente in rocce vulcaniche della vicina Provincia Magmatica Romana. Le dettagliate analisi geochimiche indicano che le rocce vulcaniche del complesso di Bolsena, presenti vicino al sito archeologico di Scoppieto, sono probabilmente il materiale vulcanico di partenza usato come componente refrattaria nelle ceramiche studiate.

1. Introduction

The archaeological site of Scoppieto is located near Baschi (Terni, Italy) and is superimposed on an Italic temple, of which several pieces of evidence still exist. It is an important archaeological centre for the study of Roman ceramic production as revealed by the remains of the kiln and all other parts for the preparation of clays and working of ceramic wares (Nicoletta, 2003). The discovery in several parts of Europe, as testified from signed tools, of a large number of lamps in *Terra Sigillata Italica* from Scoppieto, suggests that the site was important in the production of this class of ceramics from the I to the II centuries A.D. The congenial position of the site also probably led to efficient trade, as ceramic products may have reached Rome and were then distributed to the Mediterranean basin thanks to the navigable river (Tiber), easily accessible from the port of Pagliano (Olcese, 2003).

The level of specialization of the Scoppieto potters was very high - as revealed, for instance, by the findings of seals and moulds for ceramic decorations. In addition, the engravings on the objects are very complex and diverse, indicating a high level of ability of clay-working procedures.

The production of the *Terra Sigillata Italica* after an apex period of great development suddenly declined in the I century A.D., due to a sudden fall in the numbers of slaves and the start of ceramic trade from the Roman colonies. In particular, African production of *Terra Sigillata Africana* from the II cent. A.D. exceeded Italian production. The "fingerprints" of this commercial decline are testified by the discovery of traces of a fire at Scoppieto, perhaps indicating the end of site production when the decline had already started (Bergamini, 2004).

Several tools of various ceramic classes of unknown provenance have been found in the Scoppieto production centre during excavations, including several fragments of coarse ceramics, *Opus Doliare,* pestles, and amphorae, employed as re-used artefacts. Some of these have been attributed to production predating that of *Terra Sigillata Italica*. However, it is uncertain if they were produced at Scoppieto or imported from elsewhere.

One of the most intriguing archaeological topics concerns the provenance of these re-used ceramic artefacts: did Scoppieto start by producing coarse ceramics in Roman Republic times, and did it then specialise in the production of fine ceramics during the Imperial Age, or were these ceramics re-used materials imported from other production sites?

The main aims of this work are: (i) to obtain information on manufacturing techniques and the most common problems encountered during

ceramic production processes, by comparing well-made and waste products, and (ii) to define the provenance of those ceramic fragments identified as re-used artefacts. Regarding the second aim, together with ceramic samples from Scoppieto, pyroclastic rocks outcropping in the area surrounding the archaeological site and containing most of the mineral phases observed in the ceramics, were collected and analysed.

Several techniques were applied, including optical and electron microscopy, Rietveld phase analysis, calorimetric analysis, X-ray fluorescence, and Laser ablation ICP-MS. The combined use of this variety of techniques constitutes a key approach in our understanding of the technology and provenance of the ceramic materials examined here.

2. Materials and methods

2.1 Materials

Archeometric analysis was performed on 17 ceramic fragments, selected according to type, macroscopic characteristics of pastes, and quality of final products. For each group, samples of well-made and waste products were chosen. Samples of *Opus Doliare,* both coarse- and fine-grained, and pestles, two samples of tiles and two of amphorae, were analysed (Tab. 1).

In order to compare the mineralogical features of the sampled ceramics with pyroclastic rocks outcropping in the area near Scoppieto, sections of the pyroclastic succession of the Bolsena Volcanic Complex (e.g., Pallandino and Simei, 2002) were sampled for provenance determination. In detail, two sections outcropping near Botto and Baschi were examined (Fig. 1).

2.2 Optical and electron microscopy

Preliminary examination of ceramic wares was performed on thin sections under the optical microscope, which yielded general information on texture, mineralogical phases, and a rough estimate of amorphous/crystalline material ratios. Samples were also examined under a Philips scanning electron microprobe (SEM) equipped with an energy dispersive system (EDS). Chemical analysis of the mineral phases was performed by SEM-EDS, operating at 20 kV, with a beam current of 10 nA.

Table 1 – *Archaeological classification of studied ceramic groups, with inventory numbers.*

Sample number	Inventory of state	Group	Note
1	301169	pestle	Fine ware
2	302850	pestle	Coarse ware
3	331935	pestle	Coarse ware
4	271431	Opus doliare	With sigillum
5	294970	Opus doliare	With sigillum
6	235584	Opus doliare	Fine ware
7	303794	Opus doliare	Potlid
8	178759	Opus doliare	Corse ware
9	301411	Opus doliare	Corse ware
10	259947	Opus doliare	waste
11	226657	Opus doliare	waste
12	294695	Opus doliare	waste
13	351374	Opus doliare	Corse ware
14	270095	tile	waste
15	262893	tile	Well-made
16	353533	amphora	Well-made
17	353263	amphora	waste

2.3 XRD-Rietveld analysis

Quantitative analysis of the mixture of crystalline phases was greatly extended by Rietveld analysis of X-ray powder diffraction data using individual scale factors (e.g., Bish and Post, 1993). The Rietveld scale factor is correlated to the amount of each phase present in the sample by the following ratio:

$$\%i = 100\ s_i(ZMV)_i/\Sigma\ s_i(ZMV)_i$$

where %i is the weight per cent of phase i, s_i is the refined Rietveld scale factor, Z is the number of formula units per unit cell, M is the mass of the formula unit, and V is the volume of the unit cell. The equation is based on the assumption that all components in the mixture are crystalline but, when amorphous materials are also present, a crystalline internal standard must be added to the sample, in order to obtain absolute weight fractions. The following equation yields the absolute concentration of the i-th phase:

$$\%i^* = 100\ (\%i/100\text{-}\%(IS)_{added}),$$

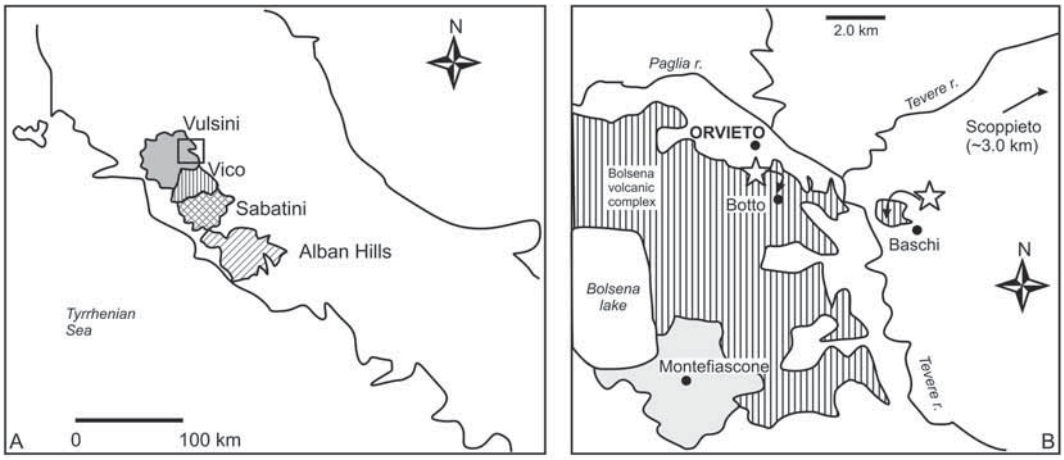

Fig. 1 – A) Location map of volcanoes in Roman Magmatic Province; B) Geological sketch-map of Scoppieto area, with location of pyroclastic rocks from Botto and Baschi sampled in this work. Major volcanic deposits constituting Bolsena Volcanic Complex also shown. White stars: sampling locations.

where $\%(IS)_{added}$ is the weight per cent of the internal standard (IS). Our samples were prepared with 10% of metallic Si.

Diffraction patterns were recorded at the Department of Earth Sciences, University of Perugia, on a Philips PW1830 with CuK_{α} radiation and a graphite mono-chromator. Patterns were collected in the 2θ range from 5º to 140°, with a scanning step width of 0.2° and a 10 sec counting time per step.

All crystalline phases present were identified and included in the model for full-profile refinement by a GSAS computer package (Larson and Von Dreele, 1986). Scale factors, background, zero shifts, peak profiles and cell parameters were refined; atomic parameters were not refined. The pseudo-Voigt profile function of Thompson *et al.* (1987) was used to fit the experimental pattern and quantitative calculations for phase analysis were then performed. The results are listed in Table 2.

Table 2 – *Mineralogical phases (in weight per cent) from Rietveld analysis. Amorph. Amorphous phase; Phyllos Phyllosilicates; other symbols from Kretz (1983).*

Sample Number	Amorph.	Qtz	Kfs	Cpx	Pl	Cal	Phyllos.	Hem
1	37	17	–	15	24	3	4	–
2	35	15	–	14	26	6	3	1
3	17	33	8	12	25	2	–	2
4	33	16	13	12	14	9	3	–
5	50	15	–	9	14	5	7	–
6	29	12	–	27	31	1	–	–
7	33	13	–	18	29	7	–	–
8	37	20	–	11	29	3	–	–
9	52	9	–	7	14	6	12	–
10	41	16	8	10	25	–	–	–
11	17	7	35	14	27	–	–	–
12	29	22	–	37	31	1	–	–
13	41	23	–	9	21	6	–	–
14	44	2	–	28	26	–	–	–
15	23	23	15	22	6	9	2	–
16	23	10	14	24	24	5	–	–
17	23	6	–	31	34	6	–	–

2.4 X-ray fluorescence

Pressed pellets were prepared by mixing a few grams of finely ground samples of ceramic body with 4 g of 12/22 lithium metaborate/tetraborate flux. A Philips PW1480 XRF system with a control program developed by Philips was employed.

Major elements [except Fe, Na and Mg, determined by wet chemical analysis, and H_2O, CO_2 and volatiles by LOI (Loss On Ignition)] were analysed by XRF, with full matrix correction according to Franzini and Leoni (1972); for minor and trace elements V, Cr, Co, Zn, Ga, Ni, Rb, Sr, Y, Zr, Nb, Ba, Ca, Pb, Ce and Th, the method of Kaye (1965) was used. Precision was better than 15% for V, Cr and Ni, better than 10% for Co, Cr, Y, Zr and Ba, and better than 5% for all other elements. Accuracy was tested according to international standards and proved to be better than 10%.

2.5. Calorimetric analysis

Thermal analyses (TG, DTG) of powdered samples were collected on a Netzsch 490C Jupiter calorimeter at the Department of Chemistry, University of Perugia. Analyses were performed in air in the temperature range 20-1000°C, at heating rate of 10°C/min.

In differential thermal analysis (DTA), the temperature difference developing between the sample and the inert reference material (Al_2O_3) was measured when both were subjected to identical heat treatment. Differential temperature was plotted against the temperature to check for any changes in samples, which led to the absorption or evolution of heat and could be detected relative to the Al_2O_3 used as standard. Fig. 2 shows representative TG, DTA and DSC curves for some samples.

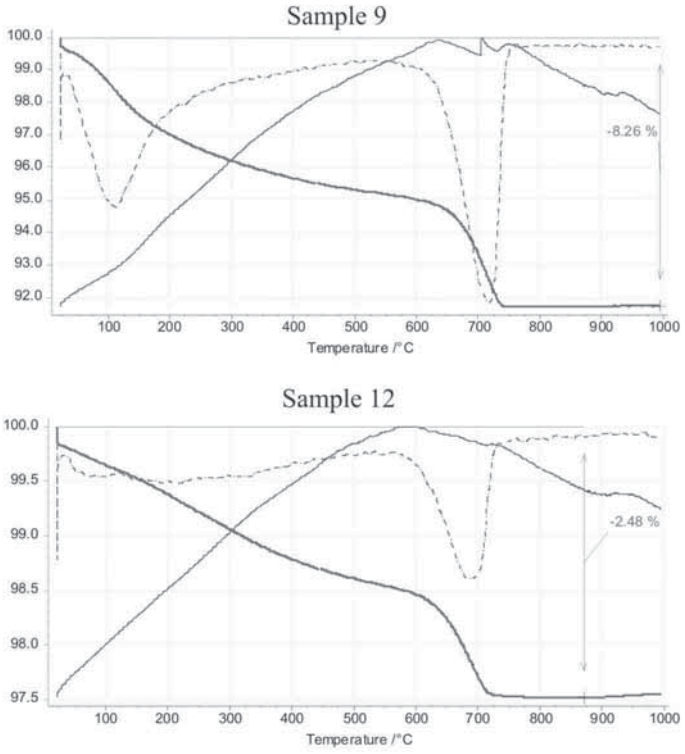

Fig. 2 – Representative calorimetric analysis: examples of good-quality product (sample 9) and waste product (sample 12). Thick line: TGA; dashed line: DTA; thin line: DSC.

2.6 Laser Ablation ICP-MS (LA-ICP-MS)

Major and trace elements were estimated by LA-ICP-MS instrumentation in the Department of Earth Sciences, University of Perugia (SMAArt facilities). The ablation system used was a commercial New Wave UP213 (New Wave, UK) frequency-quintupled Nd:YAG laser, whose fundamental emission in the infrared (1064 nm) was converted into 213 nm by means of three harmonic generators. The ICP-MS instrument was a Thermo Electron X7 from Thermo Electron Corporation (Waltham, USA), quadruple-based ICP-MS system with sensitivity of more than $6x10^7$ counts per second (cps) for 1 μg ml^{-1} of In when used in the standard solution nebulisation mode. The ICP-MS was optimised for dry plasma conditions before each analytical session on a continuous linear ablation of NIST SRM 612 by maximising signals for selected masses (La^+, Th^+) and reducing oxide formation by minimising the ThO^+/Th^+ ratio.

All LA-ICP-MS measurements were carried out using time-resolved analysis, operating in a peak jumping mode (one point per mass peak with 15 ms of dwell time), and a total of 29 elements were quantified. External calibration was performed by NIST SRM610. Helium was preferred to argon as a carrier gas, to enhance the transport efficiency of the ablated material (Eggins *et al.*, 1998). The helium carrier was mixed with the argon make-up gas downstream of the ablation cell and before entering the ICP torch, thus allowing a stable, optimal excitation condition to be maintained. Spot size was 40 μm, at a laser frequency of 10 Hz and an energy density on the sample surface of 10 J/cm^2. Complete mineral characterisation (major and trace elements) was achieved in two steps. First, major element concentrations were quantified by normalising to 100 wt.% element oxides (Leach and Hieftje, 2000, Pettke *et al.*, 2004). Second, trace elements were quantified by the method of Longerich *et al.* (1996), with a drift correction applied to unknowns and Ca as internal standard.

3. Results

3.1 Ceramics

Petrographic observation of the samples revealed peculiar features characterising the various ceramic groups. In thin section, the mixtures of *Opus Doliare* and pestles were very coarse, and fragments of chamotte used as refractory components were sporadically recognisable, whereas tiles and amphorae had a more fine-grained mixture. The latter had homogeneous grain-size, with quartz sometimes the only identifiable mineral phase. Instead, porosity, both primary and secondary, changed sharply from sample to sample, as did amorphous contents.

All samples of *Opus Doliare* and pestles revealed mineral phases of clear igneous origin, such as clinopyroxene, olivine, sanidine, leucite, and minor amphibole and biotite, probably added as skeleton. Most of these minerals are still euhedral (i.e., clinopyroxene, sanidine, leucite) and display poorly resorbed structures, indicating that the minerals were employed without hand treatment. In the waste products, biotite crystals show evident breakdown phenomena, with Ca zoning patterns, as evidenced by SEM-EDS analyses, and swelling–like separation of stacking layers (Fig. 3A), whereas in well-worked products the biotite crystals appear without thermal alteration features (Fig. 3B). Calcite crystals are still observed only in some well–worked samples, without clear evidence of pseudomorphs or burial textures.

Bulk chemical analyses of all sample wares are given in Table 3. On the ACS diagram (Fig. 4), all ceramics plot between the region of Ca-poor/Ca-rich clays as defined in Messiga (2002). However, some major chemical components (Tab. 3) show significant variations in the various samples. As a first approximation, these variations may reflect the fact that the samples belong to heterogeneous ceramic classes characterised by the sporadic occurrence of skeletal materials added to the clay and/or potential loss of volatiles (H_2O, CO_2) during firing, which may have affected major oxides. In these conditions, major element analyses can probably only provide general information and cannot be used to constrain the original composition of the mixture. Instead, trace elements can be used to compare the different samples, since they were probably little affected by the firing process. Fig. 5 shows the trace element spider diagram for all studied samples and reveals the clear-cut similarity between well-made and waste products, as well as between coarse and fine wares. These results argue

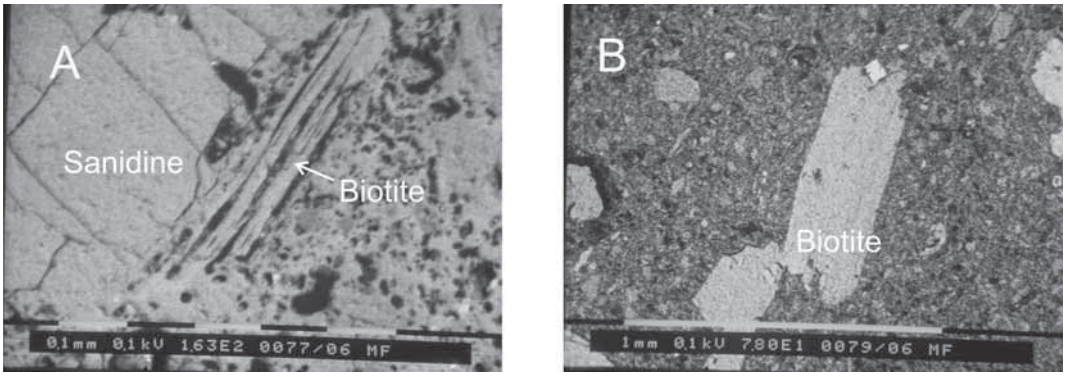

Fig. 3 – Secondary electron images of biotite from samples 11 (A) and 9 (B). In sample 9, mineral appears well crystallised; in sample 11 dehydration texture is clear-cut.

in favour of the hypothesis that similar initial mixtures were used.

More indications on production technology were pursued by studying quantitative mineralogical associations, because it is well-known that the same chemical compositions may give different paragenesis, depending on temperature. High-resolution XRD spectra were therefore recorded for all samples, for quantitative information by Rietveld analysis. Several differences emerged (Table 2): among major mineral phases, quartz varies between 2% and 33%, K-feldspar between 0% and 35%, plagioclase between 3% and 9%, and clinopyroxene between 9% and 37%. Minor mineral phases are composed of calcite (up to 9%) and a phyllosilicate (up to 12%). Amorphous contents range from 17% to 50%.

Rietveld analysis also indicates a general similarity in phase contents between good-quality and waste ware. It is noteworthy that calcite and phyllosilicates are present only in the good-quality articles but they are always absent in the waste products. Thermogravimetric and calorimetric analyses (TG, DTA, DSC) were performed on most of the samples, for additional information on firing temperature. Representative diagrams are shown in Fig. 2. Some features are common to the spectra of all samples: in the TG curve, two inflection points are observed, which correspond to two peaks in the DTA curve at 100° and 750 °C, whereas there is a continuous decrease in the TG curve in the range 100-750 °C. This is attributed to loss of adsorbed water at 100 °C and a continuous loss of hydrolysis water between 100 and 700 °C, probably associated with burial, and loss of reticular water and/or breakdown of some phases at about 750°C.

Comparisons of TG data with Rietveld analysis show good correlations between the contents of calcite and phyllosilicates and the amount of weight loss at about 750°C. These results indicate that weight loss was probably associated with the breakdown of calcite, and/or dehydration of biotite and clay minerals. It was also observed that, in the well-made products, weight loss changes from 5% to 8% in all types of ceramics, whereas it falls to 0.5-1% in waste products, with a marked decrease in calcite and phyllosilicates as already shown in the XRD refinements.

3.1 Pyroclastic rocks

The juvenile scoriaceous and pumiceous samples from Botto and Baschi, are composed of clinopyroxene, olivine, sanidine and analcimized leucite; in some cases, unaltered leucite crystals were also identified. The abundance of those minerals is different in the two sampled sites, the Botto rocks being richer in ferromagnesian minerals (clinopyroxene, olivine). Qualitatively, the mineralogical assemblage found in the sampled volcanic rocks is very similar to that found in the ceramic samples. For more detailed information on the provenance of the materials, we focused on clinopyroxene, as it is the most abundant igneous mineral in ceramics. In addition, in both ceramics

Table 3 – *XRF bulk chemical analysis of major elements (in wt%) and trace elements (in ppm) of ceramic bodies.*

Sample number	SiO_2	TiO_2	Al_2O_3	Fe_2O_3	MnO	MgO	CaO	Na_2O	K_2O	P_2O_5	LOI	V	Cr	Co	Ni	Cu	Zn	Ga	Rb	Sr	Y	Zr	Nb	Ba	La	Pb	Ce	Th
1	51.00	0.71	16.10	6.52	0.13	3.80	10.62	0.66	2.42	0.35	7.68	94	157	100	79	43	115	21	114	350	31	148	17	564	40	23	67	19
2	51.93	0.68	15.48	6.25	0.14	4.06	10.17	1.09	3.18	0.31	6.71	98	196	48	56	33	95	19	175	458	31	193	15	727	57	33	122	25
3	56.84	0.73	16.24	6.45	0.18	2.97	8.89	0.81	2.32	0.30	4.28	94	122	115	76	40	103	22	157	296	48	198	18	573	53	35	110	20
4	48.95	0.62	14.63	5.53	0.10	3.85	12.40	1.12	2.92	0.25	9.62	97	110	93	69	33	89	19	191	447	27	176	16	758	47	33	105	17
5	52.35	0.75	17.64	6.93	0.14	2.74	7.49	0.99	2.64	0.21	8.14	120	91	140	65	38	101	22	240	497	39	240	20	1050	73	45	163	31
6	52.05	0.70	16.37	6.69	0.13	4.81	11.74	1.20	2.06	0.25	4.00	89	137	84	69	36	100	24	127	495	33	218	18	606	56	40	128	32
7	50.09	0.71	15.62	6.47	0.13	3.84	13.30	0.77	2.36	0.25	6.45	95	141	47	66	46	101	21	142	391	36	175	18	761	55	27	95	21
8	56.42	0.67	16.29	6.43	0.15	3.13	10.13	0.73	2.11	0.17	3.77	112	138	53	73	56	102	20	146	314	46	172	18	488	63	27	103	19
9	48.61	0.88	21.39	7.56	0.26	1.68	8.27	0.42	2.40	0.26	8.27	204	104	88	95	70	107	23	264	486	69	369	27	1353	173	87	283	62
10	61.73	0.63	16.52	5.80	0.13	2.57	6.39	1.28	3.33	0.15	1.47	104	118	61	59	78	94	18	157	441	32	203	15	859	45	32	117	18
11	61.50	0.63	16.29	5.83	0.13	2.59	6.51	1.25	3.30	0.15	1.83	103	116	74	59	78	111	18	155	434	32	199	15	833	49	32	111	18
12	52.68	0.70	15.63	6.74	0.13	4.38	13.76	1.09	2.34	0.19	2.36	121	176	48	85	66	113	23	135	500	26	164	19	521	40	23	82	18
13	55.31	0.69	15.40	6.20	0.15	2.62	9.62	0.71	2.28	0.21	6.80	95	123	98	68	50	91	20	135	305	38	188	21	560	45	30	107	19
14	55.14	0.68	15.09	6.12	0.11	4.44	13.13	1.03	2.60	0.19	1.46	105	158	56	76	52	113	20	124	373	27	139	15	417	38	20	57	10
15	52.51	0.69	15.86	6.05	0.11	3.59	10.75	0.97	2.34	0.22	6.91	82	116	65	71	41	93	22	141	285	30	187	16	605	46	28	77	18
16	51.43	0.65	14.68	5.75	0.11	3.48	13.99	0.74	2.36	0.22	6.59	96	141	59	75	36	73	20	131	385	27	134	16	515	37	16	74	15
17	52.88	0.68	15.11	6.20	0.14	3.45	13.96	0.78	2.16	0.21	4.45	114	144	84	78	60	96	22	134	416	26	153	16	473	45	18	76	20

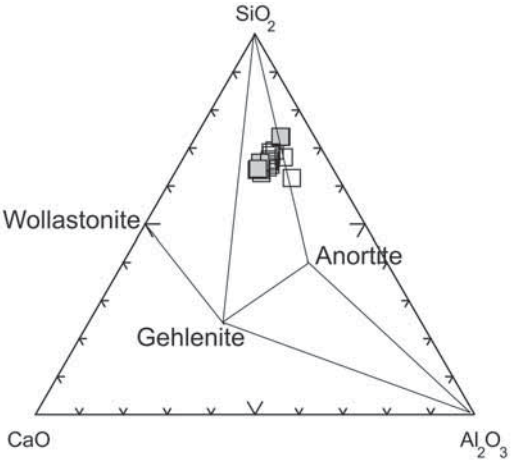

Fig. 4 – ACS diagram with mineral stability fields, including products examined here. Open squares: good-quality products; full squares: waste products.

and natural samples, clinopyroxene is the only igneous phase, that may potentially contain large, and variable amounts of trace elements. Therefore it is a good candidate as a tracer in deciphering the provenance of the volcanic materials used in the Scoppieto ceramics. A number of crystals in both ceramic and natural samples were analysed for their major and trace element contents. Results are listed in Tables 4 and 5.

Fig. 6 displays a Wo-En-Fs ternary diagram, plotting the composition of clinopyroxenes in ceramic and natural samples. Clinopyroxenes straddle the field of diopside and salite, showing a large overlap in compositions. There is no preferential clustering of clinopyroxenes from ceramics in any of the two compositional fields: on the contrary, crystals occurring side by side in the same sample display large compositional variability (see, e.g., samples 9 or 4). Regarding natural samples, Botto clinopyroxenes mostly cluster in the field of diopside, whereas those from Baschi range from diopside to salite, displaying large compositional variability even within the same rock sample.

Although the ternary plot of Fig. 6 is useful in visualising the main chemical features of the clinopyroxenes, it does not allow us to discriminate them satisfactorily, since compositions perforce cluster in a small region of the graph. Binary graphs reporting the variation of major oxides

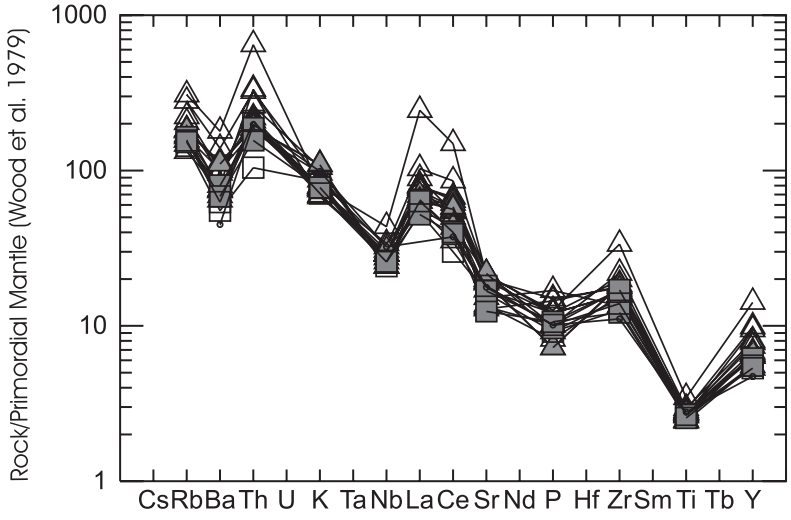

Fig. 5 – Trace element spider diagram of coarse well-made ceramics (open triangles), coarse waste ceramics (full triangles), fine well-made ceramics (open squares) and fine waste ceramics (full squares).

Table 4 – *Major and trace element contents of clinopyroxene crystals from sampled ceramics. Precision and accuracy for major elements estimated from three international reference standards (USGS BCR2, USGS BIR1, NIST612) resulting better than 6% and 10%, respectively, when concentrations are above 0.5%wt. Precision and accuracy for trace elements estimated on USGS BCR2G, resulting better than 10% for all elements.*

Element	2A	2B	2C	2D	4B	4D	4E	9A	9C	9D	9F	12A	12D	15A	15B	15C	15E
SiO_2	48.34	48.15	49.16	49.65	50.60	44.70	51.96	47.52	46.87	51.04	48.85	53.54	52.05	51.30	50.28	43.02	50.19
TiO_2	0.70	0.90	0.58	0.65	0.64	1.21	0.37	0.99	1.12	0.58	0.59	0.17	0.34	0.46	0.57	1.10	0.43
Al_2O_3	4.34	5.49	4.55	6.04	4.64	9.46	2.12	6.07	7.33	3.42	4.05	1.38	2.62	2.90	3.84	7.64	3.00
FeO	8.30	7.32	6.76	8.84	4.16	8.43	4.12	8.21	9.02	4.34	6.10	2.41	3.13	6.04	5.67	11.99	6.24
MgO	14.17	13.95	15.21	12.58	15.51	11.34	16.42	13.48	12.24	16.40	15.33	18.62	17.46	15.34	16.30	11.13	16.35
CaO	24.15	24.19	23.74	22.22	24.44	24.86	25.01	23.74	23.42	24.22	25.07	23.88	24.39	23.96	23.35	25.11	23.78
Tot	100.00	100.00	100.00	100.00	100.00	100.00	100.00	100.00	100.00	100.00	100.00	100.00	100.00	100.00	100.00	100.00	100.00
Wo	48.06	49.12	47.37	47.65	49.63	52.77	48.99	48.63	49.39	48.05	49.08	46.23	47.72	47.93	46.33	50.55	46.32
En	39.24	39.43	42.24	37.54	43.81	33.48	44.76	38.41	35.92	45.28	41.75	50.14	47.54	42.70	44.99	31.18	44.32
Fs	12.69	11.45	10.40	14.81	6.56	13.75	6.25	12.95	14.69	6.66	9.17	3.63	4.75	9.37	8.69	18.27	9.36
Sc	95	114	70	62	96	38	92	44	73	103	81	64	88	68	104	43	90
V	234	283	194	250	164	260	73	267	266	104	138	63	114	169	220	374	143
Mn	3246	1017	1049	1647	787	993	460	1136	1082	597	848	435	518	1150	968	1827	859
Co	28	44	35	37	37	32	41	42	37	27	35	22	28	42	35	31	36
Zn	87	24	31	56	22	40	12	54	34	17	25	14	13	30	26	70	21
Ga	11	9	7	10	7	16	3	16	14	5	6	2	3	6	7	17	6
Sr	194	239	148	189	149	408	265	427	383	251	320	148	159	178	141	456	186
Y	68	24	22	39	23	25	6	32	37	15	20	4	9	21	26	58	14
Zr	230	269	133	794	131	394	44	460	532	118	174	8	33	89	106	422	67
Nb	0.39	0.41	0.11	0.43	0.15	0.73	0.08	0.64	0.71	0.07	0.17	bdl	0.05	0.08	0.23	0.87	0.05
La	46	16	12	25	10	26	6	32	35	12	15	2	5	10	13	85	8
Ce	149	55	38	79	37	86	21	112	115	40	50	9	19	40	47	263	31
Pr	25	9	7	13	7	13	4	18	19	7	9	2	3	7	8	33	5
Nd	130	53	35	66	40	68	20	88	104	39	48	9	18	40	46	162	29
Sm	33	13	8	16	11	16	5	21	25	10	12	2	5	11	11	36	8
Eu	5.4	2.5	1.7	2.9	2.3	3.3	1.0	4.7	5.2	2.0	2.5	0.5	0.9	2.3	2.4	7.4	1.7
Gd	23.4	9.5	6.5	11.3	8.3	10.4	3.4	15.2	17.8	7.1	9.3	1.7	3.9	8.2	9.9	24.4	6.4
Tb	3.3	1.2	0.8	1.6	1.1	1.3	0.4	1.8	2.3	0.9	1.2	0.2	0.4	1.1	1.2	3.1	0.8
Dy	15.6	5.5	4.7	8.9	5.7	6.2	1.6	8.2	10.9	4.0	5.4	1.0	2.0	5.1	6.1	14.0	3.8
Ho	2.7	0.9	0.8	1.5	0.9	1.0	0.2	1.3	1.6	0.6	0.8	0.1	0.4	0.8	1.1	2.4	0.6
Er	6.5	2.1	2.1	3.7	2.0	2.4	0.5	2.3	3.7	1.3	1.9	0.4	0.8	2.1	2.4	5.6	1.3
Tm	0.77	0.27	0.26	0.53	0.22	0.28	0.06	0.34	0.41	0.15	0.20	bdl	0.10	0.26	0.31	0.62	0.18
Yb	5.4	1.9	1.9	3.4	1.4	1.9	0.3	2.0	2.7	1.1	1.4	0.3	0.5	1.6	1.7	4.0	0.8
Lu	0.78	0.25	0.23	0.50	0.21	0.25	0.07	0.30	0.35	0.16	0.21		0.07	0.21	0.26	0.59	0.13
Hf	9.5	12.1	5.0	27.5	6.2	14.2	2.6	17.5	22.6	6.0	7.9	0.3	1.8	4.0	5.4	16.4	3.6
Ta	0.05	0.10	0.05	0.11	0.02	0.12	bdl	0.47	0.14	0.03	0.02	bdl	bdl	0.01	0.06	0.15	0.02
Pb	2.0	0.4	0.3	0.8	0.6	1.5	0.6	2.1	1.0	0.6	0.7	0.4	0.3	0.3	0.5	1.7	0.2
Th	1.1	0.8	0.6	1.3	0.6	1.1	0.1	1.6	2.0	0.6	0.5	bdl	0.2	0.3	0.6	7.5	0.3
U	0.10	0.06	0.07	0.20	0.05	0.09	0.01	0.91	0.17	0.04	0.04	bdl	0.01	0.03	0.05	0.74	0.04

TABLE 5 – *Major and trace element contents of clinopyroxene crystals from Botto (BT) and Baschi (BS) pyroclastic rocks. Precision and accuracy for major elements estimated on three international reference standards (USGS BCR2, USGS BIR1, NIST612) resulting better than 6% and 10%, respectively, when concentrations are above 0.5%wt. Precision and accuracy for trace elements estimated on USGS BCR2G, resulting better than 10% for all elements.*

Element	BS01C	BS01D	BS03A	BS03B	BS03D	BT06A	BT06B	BT06C	BT06F
SiO_2	47.44	48.34	45.54	51.66	47.84	49.83	52.12	52.02	54.46
TiO_2	0.82	0.96	1.25	0.24	1.25	0.60	0.26	0.24	0.20
Al_2O_3	5.64	5.24	6.67	1.73	5.27	4.74	2.30	2.50	2.01
FeO	9.62	9.97	10.80	2.15	10.61	3.74	2.51	2.35	2.39
MgO	12.46	12.34	10.42	17.59	10.86	16.17	17.88	18.18	18.19
CaO	24.02	23.15	25.32	26.63	24.17	24.92	24.91	24.71	22.75
Tot	100.00	100.00	100.00	100.00	100.00	100.00	100.00	100.00	100.00
Wo	49.26	48.18	52.63	50.48	50.88	49.53	48.15	47.68	45.57
En	35.55	35.75	30.13	46.39	31.81	44.73	48.10	48.82	50.69
Fs	15.19	16.07	17.24	3.13	17.31	5.74	3.75	3.50	3.75
Sc	54	32	22	81	23	65	89	70	52
V	269	326	335	58	395	108	117	80	128
Mn	2601	2590	4340	420	5816	576	559	513	494
Co	26	35	22	24	22	27	27	22	20
Zn	79	87	150	14	187	17	15	16	12
Ga	12	15	19	2	18	8	3	4	3
Sr	253	380	241	166	110	185	205	190	136
Y	71	58	84	7	69	16	9	9	6
Zr	535	553	914	22	923	100	25	20	11
Nb	0.93	1.21	2.18	0.05	2.37	0.13	0.38	0.06	Bdl
La	61	65	85	6	78	9	8	5	3
Ce	180	217	251	18	252	34	21	15	13
Pr	29	31	39	3	37	6	3	3	2
Nd	151	149	197	18	177	34	17	15	11
Sm	36	31	44	5	39	9	5	4	3
Eu	6.3	6.4	7.7	1.0	6.6	1.7	0.9	0.9	0.6
Gd	26.2	22.9	32.1	3.4	25.7	6.4	3.3	3.0	2.4
Tb	3.4	3.0	3.8	0.4	3.5	0.8	0.4	0.5	0.3
Dy	16.6	15.0	19.9	1.7	16.4	4.1	2.1	2.3	1.7
Ho	3.0	2.4	3.3	0.3	2.7	0.7	0.3	0.4	0.2
Er	7.4	5.6	8.4	0.6	7.1	1.6	0.8	0.9	0.6
Tm	0.98	0.75	1.06	0.06	0.95	0.22	0.09	0.11	0.07
Yb	6.1	5.3	7.9	0.4	7.2	1.4	0.5	0.6	0.5
Lu	0.91	0.66	1.29	0.06	1.12	0.19	0.09	0.08	0.07
Hf	20.2	19.6	29.8	1.3	29.9	4.4	1.3	0.8	0.6
Ta	0.17	0.21	0.33	bdl	0.32	0.02	0.02	0.01	bdl
Pb	2.6	3.5	4.0	0.6	5.4	0.5	2.5	0.6	0.4
Th	2.2	2.9	2.8	0.1	3.5	0.5	1.5	0.1	0.1
U	0.22	0.42	0.31	0.01	0.54	0.07	0.33	0.01	0.02

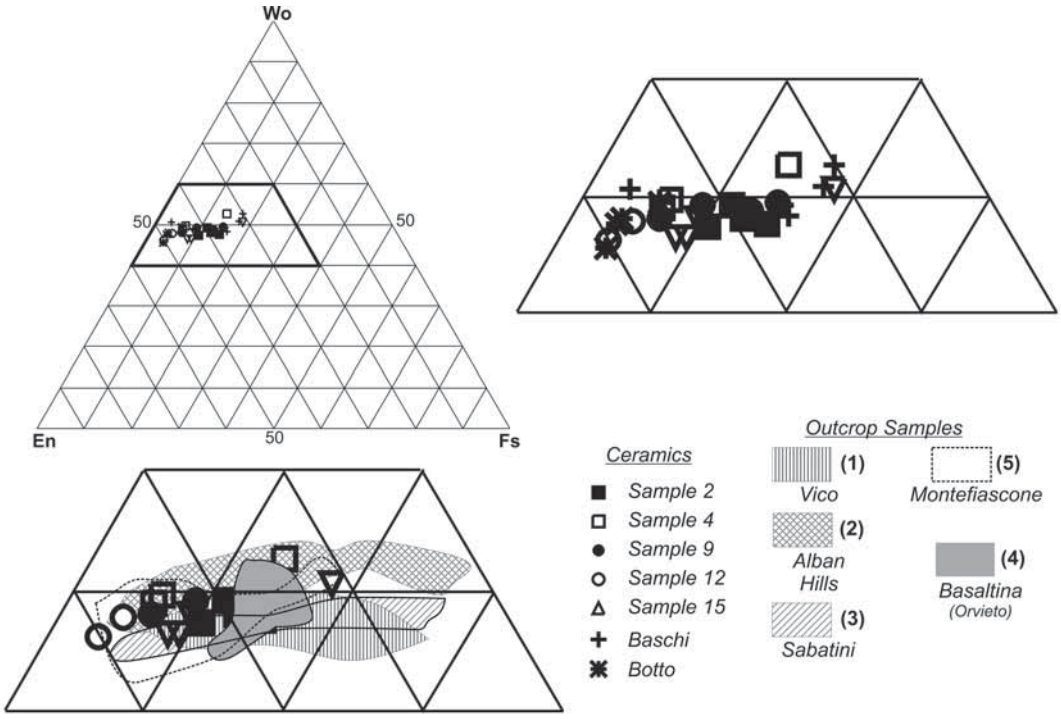

Fig. 6 – Wo-En-Fs ternary plot, showing main geochemical characteristics of clinopyroxenes from studied ceramics and natural samples. For comparison, clinopyroxenes from rocks of Roman Magmatic Province are also shown. Data of clinopyroxene crystals from Roman Magmatic Province are as follows: Vico (Perini *et al.*, 2000; 2004); Alban Hills (Aurisicchio *et al.*, 1988); Sabatini (Dal Negro *et al.*, 1985); Montefiascone (Di Battistini *et al.*, 1998); Orvieto "Basaltin" (leucite bearing rocks of tephritic to phonolitic composition outcropping as lava flows around Orvieto; Querci, 1995).

against CaO were therefore constructed. Two of them, CaO *vs.* SiO_2 and CaO *vs.* FeO_{tot}, are given in Figs. 7 and 8. They clearly show that the composition of clinopyroxene samples from Botto and Baschi (shaded area in figures) always overlap with crystals occurring in ceramics, covering their entire compositional variability.

More information on the provenance of volcanic materials used in the production of ceramics may be obtained from the trace element composition of clinopyroxenes. The trace element variability of our analysed samples is given in the spider diagram of Fig. 9A and in the REE pattern plot of Fig. 9B. The compositional variability of clinopyroxenes in the Botto and Baschi rocks is shaded in both plots, to improve graph legibility. Results indicate that the trace element variability of clinopyroxenes in the ceramics is identical to that of natural samples.

4. Discussion

4.1 Technology

Several authors (e.g., Messiga, 2002) have estimated ceramic firing temperatures using physico-chemical properties of minerals as well as peculiar mineralogical associations. During the firing of natural clays, chemical and morphological processes give rise to the breakdown of some phases and the formation of new ones, as well as shrinkage/expansion of body and intergranular bridging. Unfortunately, not only firing temperature but also clay chemical composition, especially the

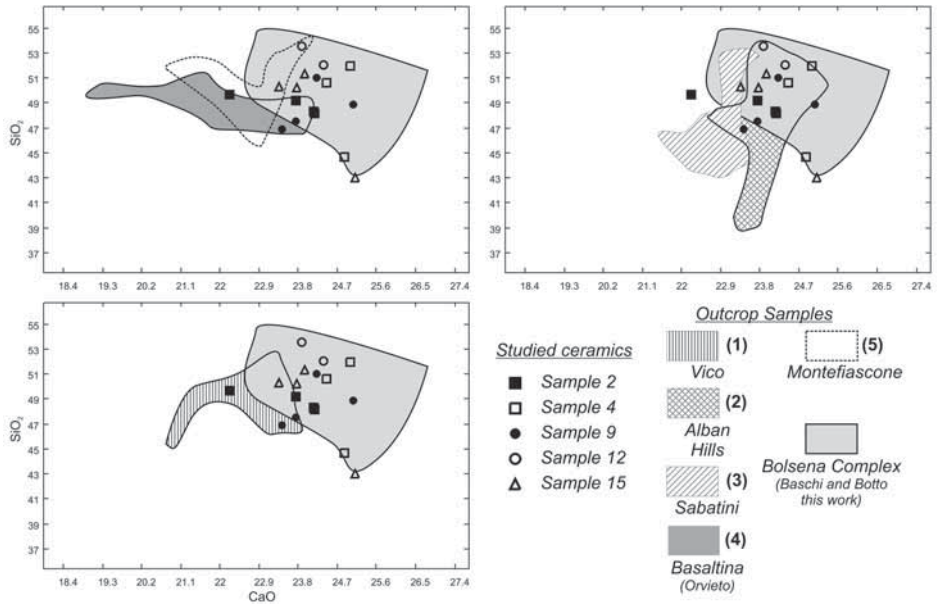

Fig. 7 – CaO *vs*. SiO_2 binary graphs, showing compositional variability of clinopyroxenes in studied ceramics and natural samples, compared with mineral chemistry of same phase from rocks of Roman Magmatic Province.

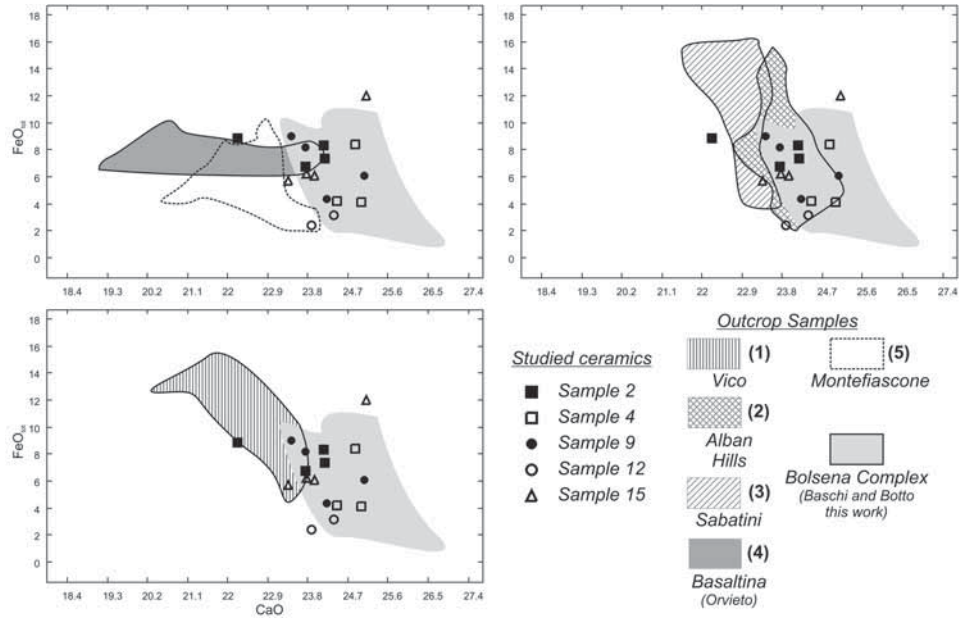

Fig. 8 – CaO *vs.* FeO_{tot} binary graphs, showing compositional variability of clinopyroxenes in studied ceramics and natural samples, compared with mineral chemistry of same phase from rocks of Roman Magmatic Province.

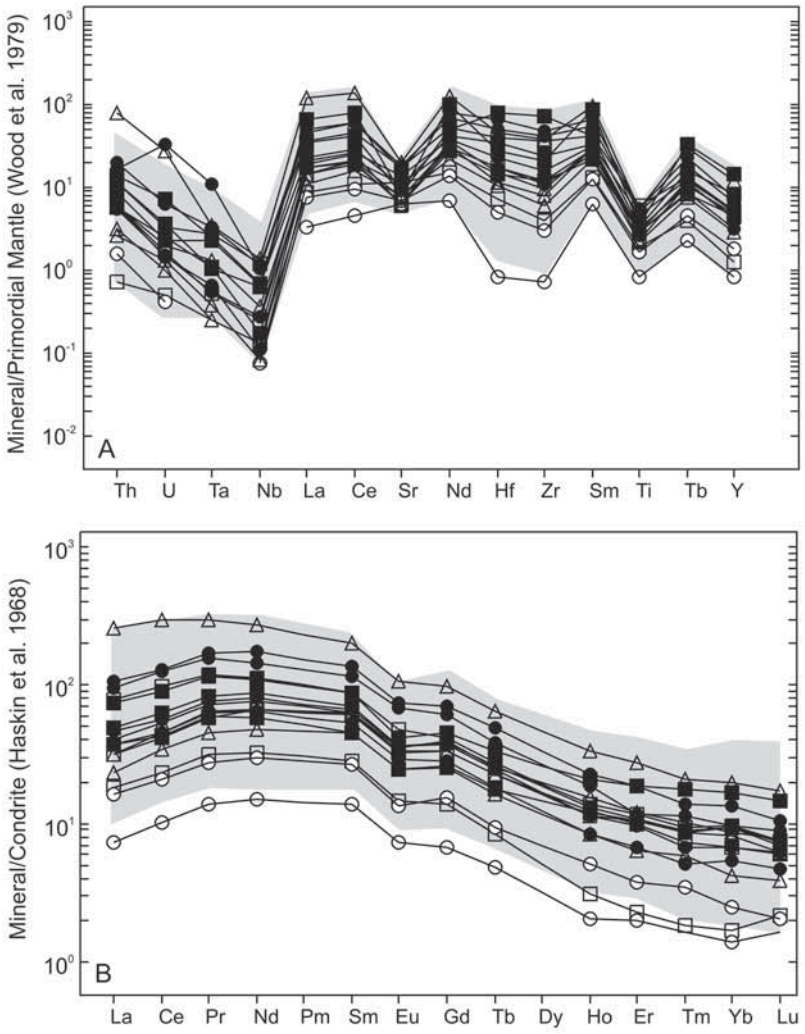

Fig. 9 – Trace element spider diagram (A) and REE patterns (B) of clinopyroxenes from ceramics compared with clinopyroxene samples from pyroclastic rocks sampled at Botto and Baschi (shaded area). Symbols as in Fig. 6.

Ca/Si ratio, can strongly influence mineralogical assemblages and, their interpretation may therefore remain ambiguous.

The extensive reactions occurring between 650 and 1000 °C involve mineral breakdown and phase reactions between carbonates and silicates, leading to the formation of gehlenite, anorthite and wollastonite/diopside (Mumenthaler *et al.* 1995). Phyllosilicates can also supply information on firing temperature, because they undergo optical and chemical changes when heated. In particular, between 550 and 850 °C, biotite loses its birefringence and pleochroism, and muscovite becomes pale yellow in colour but keeps its birefringence; biotite in contact with calcite gives rise to a Ca zoning pattern (Messiga, 2002). Our phyllosilicates also showed a K deficiency in SEM analysis. Riccardi *et al.* (1999) have already

emphasised the fact that reactions involving clay minerals, e.g., illite, imply K release from the system, with migration of the K component to a fluid phase, and solid-state diffusion of K cation into the albite phase.

In the studied samples, the chemical composition of good-quality and waste samples indicates a close analogy in the distribution of minor elements. However, our multi-method approach gave several indications of a low firing temperature for the well-made artefacts, probably under 800 °C, whereas waste products seem to be associated with an error in firing. That is:

– in well-made artefacts, calcite is found by Rietveld analysis in large percentages up to 9%, and SEM analysis revealed well crystallised minerals and not only relict phases; biotite was found in several well-made samples, with conserved optical features, with no Ca zoning or K deficiency (Fig. 3);

– Rietveld analysis does not reveal any neoformation phases, such as gehlenite or anorthite due to destabilisation of clay minerals and calcite. Only in a rare case, sample 2, did SEM show the presence of gehlenite, which forms at around 850 °C (Mumenthaler *et al.* 1995);

– Calorimetric analyses of both coarse and fine well-made artefacts show large-scale weight losses (5-10%) in the temperature range 700 - 750 °C, probably associated with the breakdown of calcite and phyllosilicates, as indicated also by XRD. Although the absolute temperature of thermal analysis may depend on rate heating and must be considered with care, firing temperatures were probably lower than those of calcite and phyllosilicate breakdown;

– Several pieces of evidence indicate that waste products are associated with temperatures higher than those of good-quality samples. In fact, calcite is not present and biotite, when present, appears with a breakdown structure (Fig. 3), K-deficient and in some cases with Ca zoning. Generally amorphous contents are higher than in well-made items and a very small weight loss (less than 1%) in thermal analysis is recorded.

4.2 Provenance

Although at first approximation results on major and trace elements lead us to hypothesise that the volcanic materials outcropping near Scoppieto were used in the production of ceramic objects, it should be noted that the igneous mineral phases identified in the ceramics are generally consistent with the mineralogical features of rocks outcropping throughout the Roman Magmatic Province.

The clinopyroxene compositions of volcanic rocks of the Roman Magmatic Province, plotted in the same graph of Fig. 6, indicate that they cover the whole range of compositional variability observed in crystals belonging to both ceramics and natural samples from Botto and Baschi. This extreme compositional variability of clinopyroxenes in these rocks has been extensively discussed in the literature, and the general consensus is that it represents the result of complex petrological processes, including mixing of magmas with differing geochemical affinities and compositions (e.g. Peccerillo, 2005).

However, when clinopyroxenes from rocks of the Roman Magmatic Province are plotted in binary diagrams (Figs. 7 and 8), several interesting features emerge. In particular, crystals from Orvieto “Basaltina”, Montefiascone, Vico and Sabatini rocks do not show major element compositions consistent with clinopyroxenes from ceramics, in that they cover only a minor segment of their compositional field. Instead, clinopyroxene compositions from the Alban Hills display a variability, which is consistent with that of the clinopyroxenes found in our ceramics. Thus, considering major elements the provenance of the volcanic materials used in the production of Scoppieto ceramics from Orvieto “Basaltina”, Montefiascone, Vico and Sabatini is not very probable; on the contrary, pyroclastic rocks from the Bolsena Volcanic Complex (Botto and Baschi) and rocks from the Alban Hills indicate suitable areas for quarrying. In this respect, the variability of trace elements may help solve this uncertainty. Unfortunately, although trace element analyses of clinopyroxene samples from ceramics and Botto and Baschi rocks were carried out in this work, no such analyses on clinopyroxenes from the Alban Hills is available in the literature. This means that further analyses will have to be performed in order to discriminate the two possible provenances.

5. Summary and conclusions

Geochemical results on clinopyroxenes strongly support the hypothesis that the volcanic materials (pyroclastic rocks) used in the production of Scoppieto ceramics belong to the Bolsena Volcanic Complex. Of course, this geochemical evidence cannot be taken as conclusive until trace element analyses on clinopyroxenes from the Alban Hills have been performed. However, the proximity of the pyroclastic outcrops of Botto and Baschi favour the hypothesis that the materials used at Scoppieto were quarried near the kiln: in archaeological contexts, the principle of "economy" is nearly always maintained. Proximity allows considerable economic savings from all aspects of craft management and was a very important factor in the ancient world, especially in ceramic production.

Additional evidence may be found from studying waste products, which usually never left their production area and thus indicate definitively local production. The Scoppieto waste products were found to have a chemical composition close to that of the well-made products, and the fact that they were unsuccessful is attributed to overheating probably due to poor control of firing temperature rather than mistakes in mixing. We may therefore conclude that, in the Scoppieto area, ceramic production had probably just began in the Roman Republican age, coarse ceramics being made with local materials and unrefined firing techniques, before the area became a very important ceramic manufacturing centre for *Terra Sigillata Italica* in the Imperial age.

Acknowledgements

We thank Riccardo Vivani for calorimetric measurements, Maurizio Petrelli for LA-ICP-MS analysis, and Luca Bartolucci for SEM observations. Stimulating comments with Pier Francesco Zanazzi, Natalia Nicoletta, and Riccardo Fani improved the quality of the paper, which also benefited of the suggestions of M.P. Riccardi, an anonymous referee and G. Vaggelli (guest editor). This work was financially supported by the University of Perugia, with funds to P.C.

References

Aurisicchio C., Federico M. and Gianfagna A. (1988) – *Clinopyroxene chemistry of the high-potassium suite from the Alban Hills, Italy*. Mineral. Petrol., **39**, 1-19.

Bergamini M. (2004) – *Scoppieto e i commerci sul Tevere*. In "Mercator Placidissimus. The Tiber Valley in Antiquity", Atti del Convegno, Roma, British School at Rome, 27-28 February, 2004.

Bish L. B. and Post J. E. (1993) – *Quantitative mineralogical analysis using the Rietveld full-pattern fitting method*. Am. Min. **78**, 932-940.

Dal Negro A., Carbonin S., Salviulo G., Piccirillo E. M. and Cundari A. (1985) – *Crystal Chemistry and Site Configuration of the Clinopyroxene from Leucite–bearing Rocks and Related Genetic Significance: the Sabatini Lavas, Roman Region, Italy*. J. Petrol., **26**, 1027-1040.

Di Battistini G., Montanini A., Bargossi G.M., Vernia L. and Castorina F. (1998) – *Petrology and geochemistry of the highly potassic rocks from Montefiascone volcanic complex (Vulsini Volcanic District, Central Italy): petrogenesis and magmatic evolution"*. Lithos, **43**, 169-195.

Eggins S.M., Kinsley L.P.J. and Shelley J.M.G. (1998) – *Deposition and element fractionation processes during atmospheric pressure laser sampling for analysis by ICP-MS*. Applied Surface Sciences, 127-129, 278-286.

Franzini M. and Leoni L. (1972) – *A full matrix correction in X-ray fluorescence analysis of rock samples*. Atti Soc Toscana Sci. Nat. Mem., A79, 7-22.

Haskin, L. A., M. A. Haskin, F. A. Frey and T.R. Wildman, *Relative and absolute terrestrial abundances of the rare earths.* In: Ahrens L.H. (ed.), Origin and distribution of the elements, vol. 1 Pergamon, Oxford, 889-911, 1968.

Kaye M.J. (1965) – *X-ray fluorescence determinations of several trace elements in some standard geochemical samples*. Geochim. Cosmochim. Acta, **29**, 139-142.

Kretz R. (1983) – *Symbols for rock-forming minerals*. Am. Mineral., **68**, 277-279.

Larson A. C. and Von Dreele R. B. (1986) – *GSAS. General Structure Analysis System*. Report LAUR-86-748. Los Alamos National Laboratory.

Leach A.M. and Hieftje G.M. (2000) – *Methods for shot-to-shot normalization in laser ablation with an inductively coupled plasma time-of-flight*

mass spectrometer. J. Anal. Atom. Spectrom., **15** (9), 1121-1124.

Longerich H.P., Jackson S.E., Günther D. (1996) – *Laser ablation inductively coupled plasma mass spectrometric transient signal data acquisition and analyze concentration calculation*. J. Anal. Atom. Spectrom., **11**, 899-904.

Messiga B. (2002) – "Reaction Path-way". In Conventional Ceramics. Proceedings of the International School Earth and Planetary Sciences in "*Engineering Mineralogy of Ceramic Materials*", Siena, 8-11 June 2001, 107-116.

Mumenthaler T., Schmitt H., Peters T., Ramseyer K. and Zweili F. (1995) – *Tracing the reaction processes during firing of carbonate-containing brick mixes with the help of catodoluminescence*. Zeit. Inter., 5/95.

Nicoletta N. (2003) – *I produttori di terra sigillata di Scoppieto*. In RCRF Acta 38, Atti del XXIII International Congress dei Rei Cretariae Romanae Fautores, Roma, American Academy, 29 settembre-6 ottobre 2002, pp. 145-152.

Olcese G. (2003) – *Terra Sigillata Italica a Roma e in area romana: produzione, circolazione e analisi di laboratorio*. Rei Cretariae Romanae Fautorum Acta, **38**, 11-26.

Palladino D.M. and Simei S. (2002) – *Three types of pyroclastic currents and their deposits: examples from the Vulsini Volcanoes, Italy*. J. Volcanol. Geotherm. Res., **116**, 97-118.

Peccerillo A. (2005) – *Plio-quaternary Volcanism in Italy: Petrology, Geochemistry, Geodynamics*. Springer-Verlag Berlin Heidelberg, 365 pp.

Perini G., Conticelli S., Francalanci L. and Davidson J.P. (2000) – *The relationship between potassic and calc-alkaline post-orogenic magmatism at Vico volcano, central Italy*, J. Volcanol. Geotherm. Res., **95**, 247-272.

Perini G., Francalanci L., Davidson. J.P and Conticelli S. (2004) – *Evolution and Genesis of Magmas from Vico Volcano, Central Italy: Multiple Differentiatiuon Pathways and Variable Parental Magmas*. J. Petrol., **45**, 139-182.

Pettke T., Halter W.E., Webster J.D., Aigner-Torres M. and Heinrich C.A. (2004) – *Accurate quantification of melt inclusion chemistry by LA-ICPMS: a comparison with EMP and SIMS and advantages and possible limitations of these methods*. Lithos **78**, 333-361.

Querci D. (1995) – *Studio di alcuni litotipi messi in opera nel Duomo di Orvieto (Terni): caratteristiche chimico-fisiche e confronto con i materiali prelevati in cava*. Unpublished Thesis, University of Perugia.

Riccardi M.P., Messiga B. and Duminuco P. (1999) – *An approach to the dynamics of clay firing*. Appl. Clay Science, **15**, 393-409.

Thomson P., Cox D.E. and Hastings J.B. (1987) – *Rietveld refinement of Debye-Scherrer synchrotron X-ray data from* Al_2O_3. J. Appl. Crystallogr., **20**, 79-83.

Wood D. A, Joron J. L., Treul M., Norry M. and Tarney J. (1979) – *Elemental and Sr isotope variations in basic lavas from Iceland and surrounding ocean floor*. Contrib. Mineral. Petrol., **70**, 319-339.